Published in final edited form as:
J Neurophysiol. 2007 January ; 97(1): 849–857. doi:10.1152/jn.00762.2006.

Contrast Affects Speed Tuning, Space-Time Slant, and Receptive-Field Organization of Simple Cells in Macaque V1

Margaret S. Livingstone and **Bevil R. Conway**
Department of Neurobiology, Harvard Medical School, Boston, Massachusetts

Abstract

We measured speed tuning of V1 cells in alert macaques to high- and low-contrast stimuli. Most V1 cells tested, both simple and complex and directional as well as nondirectional, shifted their speed tuning to slower speeds for lower contrast stimuli. We found that the space-time slant of the receptive field of directional simple cells differed for high- and low-contrast stimuli, with the space-time slant predicting higher optimum speeds for the higher-contrast stimuli; i.e., there was a larger spatial shift of the receptive-field organization per unit time. Not only did the space-time maps of directional simple cells show different slants between high- and low-contrast stimuli, but they also showed a different organization, because for high-contrast stimuli, the maps tended to show a complete inversion of the receptive-field spatial organization at long delays after stimulus onset, with initial excitation followed by suppression and initial suppression followed by excitation, but for low-contrast stimuli the receptive-field organization showed only a quadrature shift over time. We show that a simple modification of earlier models for the generation of direction-selective simple cells can account for these observations.

INTRODUCTION

Perceptual and physiological studies show that the contrast of a moving stimulus affects its apparent speed. The perceived speed of a slowly moving object is slower if it has a low contrast with its background (Dougherty et al. 1999; Stone and Thompson 1992), whereas a fast-moving object seems to move at a higher speed when its contrast is reduced (Thompson et al. 2006). The dependence of perceived speed on contrast has practical implications: for example, the high frequency of accidents under low-contrast conditions, as in fog or snow, may not be entirely due to the reduced visibility of other cars but rather to the fact that drivers think they are going slower than they actually are (Snowden et al. 1998; Stone and Thompson 1992) and therefore drive at speeds too fast for safety.

The speed tuning of cells in the motion-selective area MT shifts toward lower speeds for low-contrast (Krekelberg et al. 2006; Van Wezel et al. 2003) and low-luminance (Pack et al. 2005) stimuli. If MT cells shift to slower optimum speeds for lower-contrast stimuli and if speed information is carried by a population code in MT, then for two stimuli of different contrasts moving at the same moderate speed, the lower-contrast stimulus should appear to move faster, which is the reverse of what is observed. This discrepancy could be explained if speed information is carried by a rate code rather than a population code in MT (Krekelberg et al. 2006).

Address for reprint requests and other correspondence: M. Livingstone, Dept. of Neurobiology, Harvard Medical School, Boston, MA 02115 (E-mail: mlivingstone@hms.harvard.edu).

Although MT probably inherits its direction selectivity from V1 (Livingstone et al. 2001; Movshon and Newsome 1996; Pack et al. 2003, 2006), it is not known to what extent MT inherits its *speed* selectivity from V1. MT cells generally prefer higher speeds than V1 cells (Mikami et al. 1986) even though MT receives its predominant input from V1 (Anderson and Martin 2002; Anderson et al. 1998; Rockland 2002). Nevertheless, recent quantitative studies from our laboratory have shown that the local-motion-detection behavior of MT cells is almost indistinguishable from the behavior of direction-selective V1 cells at the same eccentricity, in terms of selectivity for both spatial and temporal features (Pack et al. 2006).

Reduced contrast may affect speed processing at a stage earlier than MT. The responses of V1 neurons vary with stimulus contrast; in particular, lower-contrast delays processing in the retina and shifts the temporal tuning in V1, in the LGN, and in the retina to lower temporal frequencies (Carandini et al. 1997; Maunsell and Gibson 1992; Maunsell et al. 1999; Reich et al. 2001; Sestokas and Lehmkuhle 1986; Shapley and Victor 1978). Lowering contrast has been reported to expand the time course of the space-time maps of directional cells in anesthetized cat and to increase direction selectivity (Peterson et al. 2006). But the effect of reducing contrast on speed tuning in V1 has not been explored. In this study, we compared the effect of lowered contrast on speed tuning in V1 to its effect on the spatial and temporal properties of simple-cell receptive fields.

In both cat and primate, directional simple cells show a systematic shift in response timing across the receptive field. That is, when responses are plotted in space-time coordinates, they are slanted in space-time. This space-time slant is thought to reflect the mechanism by which these cells exhibit direction selectivity: For example, the ON (light excitatory/dark inhibitory) responsive parts of a directional simple cell form a diagonal in space-time in such a way that the response to a white stimulus shows a longer time to peak on the side of the receptive field that a preferred-direction stimulus encounters first and a shorter time to peak on the side of the receptive field that a preferred stimulus encounters later. Therefore stimuli moving in the preferred direction encounter later peaking parts of any given subregion of the receptive field before the early peaking parts (Conway and Livingstone 2003; De Valois et al. 2000; DeAngelis et al. 1993a; McLean and Palmer 1989; McLean et al. 1994). Because of these timing differences, peak responses arising from different parts of the receptive field are synchronous for stimuli moving in the preferred direction and asynchronous for stimuli moving in the reverse, or null, direction. Because speed tuning in simple cells correlates with the space-time slant of their receptive fields (Conway and Livingstone 2003; McLean and Palmer 1989; McLean et al. 1994), we also asked whether contrast affects the spatiotemporal slant in V1 simple cells.

METHODS

Macaque monkeys were prepared for chronic recording as described previously (Conway and Livingstone 2003; Livingstone 1998, 1999). All experiments were carried out according to National Institutes of Health guidelines for the use of animals and with the approval of the Harvard Medical School Standing Committee on the use of Animals. Eye position was monitored with a search coil in a magnetic field (Judge et al. 1980) using eye-position monitors from DNI and CNC Engineering. Well-isolated single units were recorded from V1 using tungsten microelectrodes (Hubel 1957) (FHC, Bowdoinham ME) from two alert fixating macaque monkeys. Spikes were collected at 1-ms resolution; eye position was sampled at 250 Hz. Stimuli were presented on 21-in monitors with a 75-Hz refresh rate (noninterlaced). The monitor screen was 57 cm in front of the animal. The animal was rewarded for keeping his gaze within 1° of a fixation spot, and spikes were rejected from analysis if they were collected while the animal's gaze was outside this fixation window.

For all the stimuli used, the luminance of the gray background was 35 cd/m^2; the high-contrast white was 70 cd/m^2; the low-contrast white was 38.5 cd/m^2; the low-contrast black was 31.5 cd/m^2; the high-contrast black was <1 cd/m^2. Thus the contrast, defined as the difference between the luminance of the stimulus and the background as a fraction of the background luminance ($|L_{stimulus} - L_{background}|/l_{background}$), was ~100% for the high-contrast stimuli and 10% for the low-contrast stimuli.

Fields of moving bars were used to characterize each cell's direction and speed tuning. The orientation, speed, sign of contrast (against a gray background), and width of the bars were chosen to be optimum for each cell; bar length was chosen to be shorter than optimal to avoid the effects of end-stopping. The onset positions of the smoothly moving bars were random within a stimulus range that was larger than the cell's receptive field. The bar density was high enough that there was on average at least one bar in the receptive field at any time, unless the cell gave a higher sustained firing rate to a lower bar density. This stimulus is analogous to a random-dot field, which is a standard stimulus for studying speed tuning in MT; this stimulus gives higher sustained firing rates than either grating stimuli or single bars. Direction indices (DI) were calculated as: $(R_p - R_n)/(R_p + R_n)$ where R_p is the response to the preferred direction and R_n is the response to the null direction. Responses were calculated as the total spikes over the entire response minus baseline firing (the response during presentation of the background gray). The direction index for moving bars can range from 0 (for a cell that gives equal responses to the 2 directions) to 1 (for a cell that responds only to 1 direction, the "preferred" direction), and even >1 for cells that are suppressed below baseline by null-direction stimuli. Each isolated single unit encountered (n = approximately 170) was screened for directionality using moving bar fields. Cells were considered directional if in response to moving high-contrast bars they had a DI > 0.3; 43 cells met this criterion. Twenty one of these directional cells were deter-mined to be simple (Conway and Livingstone 2003; Hubel and Wiesel 1962; Tsao et al. 2003) and 22 were complex. Toward the end of the study we tested the speed tuning of 19 nondirectional complex cells. We have no reliable information as to cortical layer.

Space-time maps were generated by presenting two optimally oriented bars each frame (13 ms), one black and one white, at random positions along a stimulus range that was wider than the cell's receptive field. Low- and high-contrast conditions were run separately. We collected at least twice as many spikes for the low-contrast condition as for the high-contrast condition. Spikes were reverse correlated with the position of the bars along the stimulus range, and space-time maps were plotted as light minus dark responses, red indicating light-excitatory (ON) responses, and blue indicating dark-excitatory (OFF) responses (Conway and Livingstone 2003; Tsao et al. 2003). Maps were smoothed with a two-dimensional (2-D) Gaussian with a sigma of 9 ms in the temporal dimension and 3 pixels in the spatial dimension; average baseline was taken as the average firing from 0 to 40 ms and subtracted from these difference maps. Maps were normalized so that the largest response, ON or OFF, corresponded to the maximum of the firing-rate scale.

Tilt direction indices (TDIs), optimal spatial frequency (F_S), and optimal temporal frequency (F_T) were calculated from the 2-D discrete Fourier transform of the space-time maps. The peak of the Fourier transform (fast Fourier transform, Matlab) represents the optimal spatial (F_S) and temporal frequencies (F_T) of the 2-D Fourier transform of the space-time map. The tilt direction index (TDI) was taken as $(R_p - R_n)/(R_p + R_n)$, where R_p and R_n represent the amplitude of the 2-D FFT at (F_S, F_T) and (F_S, F_{-T}). TDIs reflect the spatiotemporal asymmetry in the space-time maps and correlate with direction selectivity (Anzai et al. 2001; Baker 2001; DeAngelis et al. 1993a).

We did not measure direction selectivity at low and high contrast using moving bar fields, but we did calculate the directionality of the responses to the sparse noise stimuli, by calculating

phi-motion direction indices (ϕDIs) from the same data that were used to generate the space-time maps (Livingstone et al. 2001). We have previously shown that for directional cells in both MT and V1, responses to pairs of sequentially presented flashed stimuli are well correlated with direction tuning to moving stimuli (Livingstone and Conway 2003; Livingstone et al. 2001; Pack et al. 2006). The average response to same-contrast sequential-frame stimulus pairs at the optimum inter-stimulus distance, in which the stimulus sequence was in the preferred direction (R_p), was compared with the average response to stimulus sequences in the reverse direction (R_n): $\phi DI = (R_p - R_n)/(R_p + R_n)$.

Space-time slant was measured in two ways. First, we fit a Gabor to the spatial map at the peak of the absolute value of the response. We used this Gabor (i.e., with all parameters except phase set to the same values of the Gabor that was fit to the peak) to find the phase of the spatial profile at each contiguous 1-ms horizontal slice of the smoothed space-time map for the duration of the response. Response onset was defined as that point in time at which the absolute value of the space-time map reached 1/*e* times the maximum absolute value of the map. Response duration was measured from the space-time maps as the length of time that the response was ≥1/*e* times the peak of the largest magnitude component, either ON or OFF, whichever was larger. The phase, relative to the phase at response onset, was plotted as a function of time after stimulus onset for the duration of the response. The slant of the space-time map was calculated from this plot by converting the phase shifts to visual angle and then calculating the linear least-squares fit. The second way we measured space-time slant was to integrate the amplitude of the 2-D discrete Fourier transform of the space-time map along each spatial-frequency/temporal-frequency orientation. We took the angle with the maximum integral as the orientation of the map.

Speed tuning was measured using fields of optimally oriented moving bars, of the same contrast, low or high, as described above, against a gray background. Stimulus duration was 3 s, and responses were averaged over that entire time, for ≥10 presentations. Optimum speed was taken as the peak of a log-Gaussian fit to the data (Nover et al. 2005; Pack et al. 2005). The r^2 values for the fit ranged from 0.57 to 0.98; median = 0.79. Low and high contrast conditions were run separately.

We modeled the responses of direction-selective simple cells and the pairs of nondirectional cells that might combine to result in directional simple cells. For this model, we used the same Gabor as the spatial profile for all components; for one of the nondirectional components the Gabor was shifted spatially from the other component a distance corresponding to [1/4] cycle of their spatial profile; i.e., the two components were in spatial quadrature. For all the biphasic temporal profiles we used a formula of the form: $f(t) = t^r * e^{-}t[r]\ [1/r! - t^2/(r + 2)!]$ where t = time and r is a constant that is increased to generate slower responses (Adelson and Bergen 1985). The monophasic temporal profiles are Gaussians. For each row in Fig. 5, the two nondirectional inputs are added together to generate a directional simple cell. Response phase was calculated in the same manner as for the real simple cells.

RESULTS

We measured speed tuning to both high- and low-contrast stimuli in 62 V1 cells—21 direction-selective simple cells, 22 direction-selective complex cells, and 19 nondirectional complex cells. Directional, as well as nondirectional, V1 cells, like MT cells (Krekelberg et al. 2006; Pack et al. 2005; Van Wezel et al. 2003), shifted their speed tuning so that the peak of the tuning curve was at lower speeds for lower contrast stimuli (Fig. 1, *A* and *B*). For some cells, the tuning curve simply shifted leftward, as in Fig. 1; other cells became low-pass for low-contrast stimuli (Fig. 2, *top* and *bottom*). All but one of the V1 cells showed a lower optimum speed for low-contrast moving bars than for high-contrast bars (Fig. 1*C*); the geometric mean

of the ratio of high-contrast optimum speed to low-contrast optimum speed was 2.6 ± 2.1 (mean ± SD) for the V1 population; for the simple cells alone, the mean ratio was 2.6 ± 1.9). Previously MT cells were found to show on average a twofold shift in preferred speed for a comparable change in contrast (Krekelberg et al. 2006; Pack et al. 2005).

It has been previously reported that in anesthetized cat both simple and complex cells become more direction selective at lower contrast (Peterson et al. 2006). We compared the degree of directionality for low- and high-contrast stimuli using responses to the space-time mapping stimulus, which consists of a series of rapid bar presentations. Each sequential pair of frames constituted an apparent motion stimulus, from which we calculated a phi-motion direction index (see METHODS). As shown in Fig. 1*D*, for our population of 43 direction-selective cells, there was no significant difference between the ϕDIs at low contrast and those at high contrast for either complex or simple cells (paired *t*-test, $P > 0.1$). Although this result is inconsistent with the study of Peterson et al. (2006), it is consistent with findings of Ledgeway et al. (2005), who reported that only a small minority of directional neurons in area 18 of the anesthetized cat showed stronger directionality to low-contrast gratings compared with high-contrast gratings.

To explore the mechanism of the contrast dependency of speed tuning, for the 21 simple cells, we also obtained receptive-field space-time maps using both high- and low-contrast bar stimuli. These maps were generated by presenting one dark bar and one light bar on an intermediate gray background in each frame at random locations along a one-dimensional stimulus range that was perpendicular to the cell's preferred orientation. The space-time receptive-field maps show activity as a function of the bar position and time after stimulus onset (Conway and Livingstone 2003); activity is mapped as light minus dark responses. Maps and speed tuning for four simple cells are shown in Fig. 2. Consistent with the population trend in Fig. 1, the speed tuning of these V1 simple cells shifted leftward, toward lower speeds, for the lower contrast stimulus (Fig. 2, *right*).

For all four cells in Fig. 2, the space-time maps are slanted. It has previously been shown for both cat and primate visual cortex that slanted space-time maps are characteristic of direction selective simple cells and that preferred direction and optimum speed correlate with this slant (Conway and Livingstone 2003;De Valois et al. 2000;DeAngelis et al. 1993a,b;McLean and Palmer 1989;McLean et al. 1994). Furthermore, in anesthetized cat, the degree of asymmetry in the space-time map correlates with, but underestimates, the directionality of the cell (Anzai et al. 2001;Baker 2001;DeAngelis et al. 1993a;Peterson et al. 2006).

We characterized several properties of the space-time maps of the simple cells to determine whether contrast-dependent changes in any specific properties might correlate with the changes in speed tuning. We measured the degree of asymmetry in the space-time maps by calculating an index comparing the amplitude of the spectrum at the optimum spatial (F_S) and temporal frequency (F_T) to the amplitude at (F_S, F_{-T}). In Fig. 3*A*, we compare this index for space-time maps generated using high- and low-contrast stimuli. As with the directionality measured by comparing responses to preferred and null-direction phi-motion stimuli, this predicted directionality index also did not show any significant difference between the high- and the low-contrast conditions (paired *t*-test, $P > 0.1$).

The speed of an object is the distance it travels per unit time; therefore selectivity for speed depends on both spatial and temporal tuning properties. Priebe et al. (2006) tested V1 cells with sine-wave grating stimuli and found that V1 simple cells are mostly not tuned for speed per se (that is, for a specific $\Delta_{space}/\Delta_{time}$), but instead speed tuning tends to vary with spatial frequency, indicating separable tuning for temporal and spatial frequency. Our nonperiodic

stimuli are complex in both spatial and temporal frequency. The observed shifts in speed tuning therefore could reflect contrast-dependent shifts in either spatial- or temporal-frequency tuning.

We did not measure spatial- or temporal-frequency tuning by comparing responses to varying spatial and temporal frequency sine-wave gratings but instead inferred the tuning from the space-time maps (DeAngelis et al. 1993a,b). Figure 3*B* shows the optimal spatial frequency of the space-time maps generated at high and low contrast for the 21 simple cells we studied, as estimated by the spatial frequency (F_S) corresponding to the peak amplitude in the 2-D discrete Fourier transform of the space-time maps. There was no significant difference between the optimal spatial frequency, as measured, of the space-time maps at the two contrasts used (paired *t*-test, $P > 0.1$).

On the other hand, there were consistent differences between the temporal properties of the responses to high- and low-contrast stimuli. It has been previously observed, for directional cells in anesthetized cat visual cortex, that responses at low contrast are expanded in time compared with responses at high contrast (Peterson et al. 2006). We examined the space-time maps of our primate simple cells for evidence of this and found that the space-time maps generated using low-contrast stimuli showed several differences compared with the high-contrast maps. Compared with the responses to high-contrast stimuli, the responses to low-contrast stimuli: began slightly later, some lasted longer, and showed a more vertical slant in space-time plots.

As a first approach to quantifying the temporal properties of the space-time maps, we determined the temporal frequency (F_T) that corresponded to the peak of the 2-D Fourier transform of each space-time map. The optimal temporal frequency for all the simple cells generated using high and low contrast is plotted in Fig. 3*C*. The optimum temporal frequency was significantly higher for high-contrast stimuli [7.2 ± 3.1 (SD) Hz] than for low-contrast stimuli (5.5 ± 2.7 Hz; paired *t*-test, $P < 0.01$).

Another way to look at the spatiotemporal properties of the simple cells is to measure the space-time slant of the maps. If direction-selective simple cells act as linear filters for detecting motion, the space-time slant of each cell should predict its tuning for speed and direction of stimulus motion (Adelson and Bergen 1985; Watson and Ahumada 1985); this has been shown to be the case for directional simple cells in anesthetized cat (Baker 2001; DeAngelis et al. 1993b; McLean and Palmer 1989; McLean et al. 1994), anesthetized primate (De Valois and Cottaris 1998; Gaska et al. 1994), and alert primate (Conway and Livingstone 2003). To find out whether the shift in speed tuning with contrast was correlated with a change in the space-time slant of simple-cell receptive-field organization, we quantified the space-time slant of all the direction-selective simple cells we recorded in two different ways (Fig. 3*D*).

First, we fit the spatial profile with a Gabor and calculated the phase of that Gabor relative to the phase at response onset. In Fig. 2, *third column*, are shown for the same four cells the relative spatial phases of the responses as a function of time after stimulus onset, for all the 1-ms epochs in which the response was larger than 1/*e* times the peak response, for high (—)- and low (- - -)-contrast stimuli. We used the slope of these plots to estimate the space-time slants of the receptive fields, in terms of degrees of visual angle per second. This estimate, or predicted optimum speed, is indicated for each cell in Fig. 2, for high and low contrasts, and is plotted for the entire simple-cell population in Fig. 3*D*, ■. The slope of the space-time maps was significantly less vertical, corresponding to faster speeds, for high-contrast stimuli than for low-contrast stimuli (paired *t*-test, $P < 0.05$).

As an alternative way to calculate the space-time slant of the simple cells we calculated the integral of the amplitude along each (spatial frequency/temporal frequency) orientation in the 2-D Fourier transform of the space-time maps. The orientation with the maximum integral for

each simple cell, for high and low contrast, is shown in Fig. 3*D* (○). The space-time slant for all of the simple cells was again significantly less vertical for high-contrast stimuli compared with low-contrast stimuli (paired *t*-test, 1-tailed, $P < 0.01$). The ratio of space-time slant at high contrast to that at low contrast was 1.7 ± 1.4 (geometric mean ± SD) for the slope of the phase plot and 1.9 ± 1.4 for the change in optimum FFT orientation. Both ratios were slightly less than the average high-contrast to low-contrast speed ratio for simple cells of 2.6 ± 1.9 (geometric mean; see preceding text). Thus speed tuning is somewhat more reduced by contrast than is the space-time slant.

The time course of the response of simple cells and their space-time slant were affected by stimulus contrast but spatial frequency tuning was not. We therefore asked whether the contrast-dependent shift in speed tuning could be predicted from the temporal-frequency tuning of the cells or from their space-time slant or both. Figure 4 shows the relationship between the actual speed tuning measured with fields of drifting bars and the speed tuning predicted from the temporal and spatiotemporal properties of the space-time maps for the 21 simple cells. In *A* is plotted the relationship between actual optimum speed and the speed tuning predicted by dividing the peak temporal frequency (F_T) by the peak spatial frequency (F_S), both derived from the location of the peak in the 2-D Fourier transform of each space-time map. There is a poor correlation (slope = 0.7; $r^2 = 0.33$). The correlation was better between the actual speed tuning and the speed tuning predicted from the space-time slant, measured either by the change in phase over time (slope = 1.05; $r^2 = 0.60$) or by the peak orientation of the 2-D FFT of the space-time map (slope = 1.01; $r^2 = 0.61$). Thus the optimum speed tuning of simple cells correlated better with their space-time slant than with the ratio of the optimum temporal frequency to the optimum spatial frequency. This is probably because our method of estimating optimal spatial and temporal frequency, indirectly from the space-time maps, was not accurate.

For both ways of measuring space-time slant there is a correspondence between the optimum speed measured with drifting fields of bars and the optimum speed predicted from the space-time slant, as previously shown (McLean and Palmer 1989; McLean et al. 1994), and there is a shift in both optimum speed tuning and space-time slant to lower speeds for low-contrast stimuli.

As shown in Fig. 2, *third column*, we calculated the spatial phase as a function of time after stimulus onset for each simple cell, at high and low contrast. For the high-contrast stimuli, the space-time maps tended to invert phase by the end of the response, so the response at a single position of the receptive field might go from ON (light excitatory, dark inhibitory) to OFF (dark excitatory, light inhibitory) over time, or vice versa (Fig. 2, *1st column*). This can be seen in Fig. 2, *third column*, as a phase shift of approximately one-half cycle, or π, over the course of the response, for the high-contrast stimuli. The space-time maps of the same cells in response to low-contrast stimuli tended not to invert completely. Similar trends were observed for the entire population of simple cells: the mean phase shift from the onset of the response to the end of the response was 0.96 ± 0.25π (mean ± SD) for high-contrast stimuli, whereas the mean phase shift for low-contrast stimuli was 0.54 ± 0.2π. Thus the total phase shift from the beginning to the end of the response tended toward π for high contrasts but tended to be closer to π/2 for low contrasts.

One might suppose that the reason the low-contrast total phase shift over the duration of the response might be smaller than the high-contrast overall phase shift is that the low-contrast stimulus generates a smaller response than the high-contrast stimulus, so the response simply subsides sooner, before reaching a complete phase reversal. Or one might propose that if we measured the terminal phase shift at a particular point in time that was the same for both contrasts, then, because the low-contrast response is temporally expanded, it might not attain its final phase configuration by that point in time. However, we defined the duration of the

response over which we calculated the phase shift as all contiguous time-points of the response for which the magnitude of the response (ON or OFF) was more than 1/*e* times the maximum of the absolute value of the magnitude of the response. Therefore the difference between the total phase shift for the two contrast conditions is not likely due to the low-contrast response being either weaker or slower (i.e., expanded over time) than the high-contrast response, but instead it seems to reflect a difference in the spatiotemporal organization of the response between high- and low-contrast conditions.

If lowering contrast simply expanded the time course of the space-time response, as previously proposed (Peterson et al. 2006), then the space-time maps should not show a systematic difference in overall phase shift between high- and low-contrast conditions. This prediction is illustrated the model diagrammed in the *first two rows* of Fig. 5; here a model for generating space-time slanted simple cells is shown with a temporally expanded version of the same model in the *second row*. The model in the *first row* is the same as originally proposed Adelson and Bergen (1985) in which two nondirectional simple cells, spatially and temporally offset from each other by [1/4] cycle are combined linearly to generate a space-time slanted simple cell. For the model in the *second row*, the time course was simply expanded. Both the original (high-contrast) version and the temporally expanded (low-contrast) version of this model show a phase shift larger than π from the beginning to the end of the response. This is to be expected because a single temporally biphasic response would show a phase shift of π from the beginning to the end (because a response inversion is a phase shift of π) and by adding a second component in spatial quadrature (i.e., with a phase shift of π /2 relative to the first component) the final phase shift should approach 1.5 π.

How can this model be modified to explain a change in both space-time slant and phase shift over time? Space-time slanted simple-cell receptive fields in both cat and monkey can be mathematically resolved into nondirectional components in which the early component is temporally biphasic, but the later component is best fit with a temporally monophasic profile (Conway and Livingstone 2003; De Valois and Cottaris 1998; De Valois et al. 2000; Peterson et al. 2004). Such a model is shown in Fig. 5, *third row*, with the time course of one component being temporally biphasic and the time course of the later component being temporally monophasic. This model generates a directional cell that shows a phase shift of π (Fig. 5*C*), which is closer to what we observed than the shift of 1.5 π predicted by a model in which both input components are temporally biphasic.

To account for the effects of lowering contrast on the slope and phase shift of the space-time maps, we assume that the effect of lowering contrast is not only to make both nondirectional components slower but also to make the biphasic component become monophasic by eliminating its rebound phase. This assumption is supported by studies showing that lowering contrast or luminance can change a biphasic response into a monophasic one: in the primate, geniculate responses become less biphasic at low contrast (Benardete and Kaplan 1999). And in cat, primary visual cortical responses become more monophasic, losing the rebound phase, at low luminance (Peterson et al. 2001; Ramoa et al. 1985). This assumption is also consistent with previous studies showing that at high-contrast visual neurons are temporally band-pass, but at lower contrast they become low-pass (Carandini et al. 1997; Purpura et al. 1990). If the rebound phase of the faster component were thus selectively decreased at lower contrast, as shown in Fig. 4*D*, lowering contrast would shift the space-time slant toward slower speeds and reduce the total phase shift from π to π/2, consistent with our observations.

DISCUSSION

Contrast affects speed tuning as early as V1 simple cells, the earliest cells in the primate geniculocortical pathway that show direction selectivity. We show here that reducing contrast

results in a reduction in the preferred speed of direction-selective simple cells, an effect that is reflected in a change in the slope of the responses plotted in space-time coordinates. The effects of contrast on speed tuning presumably contribute to similar effects previously noted in MT neurons. Because MT neurons inherit their directionality from V1 (Livingstone et al. 2001; Movshon and Newsome 1996; Pack et al. 2006), the effect of contrast on the speed tuning of MT cells therefore cannot be entirely due to mechanisms inherent in MT (e.g., loss of suppression within MT). The magnitude of the speed tuning shift we observed in V1 was comparable to that observed in MT for low-contrast (Krekelberg et al. 2006; Van Wezel et al. 2003) and low-luminance (Pack et al. 2005) stimuli and may therefore account for most, if not all, of the speed tuning shifts observed in MT.

We found that contrast also affects the space-time slant of V1 simple cells in the same direction and with about the same magnitude as it affected their speed tuning. Lowering contrast shifts the temporal properties of retinal ganglion cells and LGN cells so that they show a longer latency and lower temporal frequency tuning; i.e., they become less transient at low contrast (Maunsell and Gibson 1992; Maunsell et al. 1999; Reich et al. 2001; Sestokas and Lehmkuhle 1986; Shapley and Victor 1978). Therefore one might suppose that low contrast simply slows all visual processes, delaying all responses equally. However, it is not clear that simply slowing responses, as observed in the retina and LGN, would change the space-time slant of V1 simple cells: a change in slant would require relatively more slowing of the late components of the space-time map than of the early components, otherwise the spatiotemporal map should show the same shape, or slant, just delayed.

Our observation that at high contrast the space-time maps of directional simple cells tend to show a phase shift of π, but at low contrast they tend to show a phase shift of around $\pi/2$, indicates that the spatiotemporal receptive fields of directional simple cells change shape, not just time course, with contrast; this in turn suggests that different components making up the receptive field are differentially affected by contrast. These two observations suggest two modifications of the linear-filter model for generating space-time slanted directional simple from pairs of nondirectional inputs (Adelson and Bergen 1985; Watson and Ahumada 1985). In particular, we propose that the two nondirectional inputs consist of one temporally biphasic input and one temporally monophasic input; this idea was originally suggested based on mathematical decomposition of space-time maps of directional simple cells (Conway and Livingstone 2003; De Valois et al. 2000; Peterson et al. 2006). Our observation of a phase shift of half a cycle, or π, over time is more consistent with this new model than with the combination of two temporally biphasic nondirectional inputs. Furthermore, if we allow the temporally biphasic input to become temporally monophasic at low contrast, then we can account for both the change in space-time slant and the different phase-shift behavior over time.

We did not find the directionality of cells in macaque V1 to be increased at lower contrast. Although this result is inconsistent with the study of Peterson et al. (2006), it is consistent with findings of Ledgeway et al. (2005), who reported that only a minority of directional neurons in area 18 of the anesthetized cat showed stronger directionality to low-contrast gratings compared with high-contrast gratings. The variability of the effects of contrast on the degree of directionality may reflect the contrast dependency of surround effects rather than the contrast dependency of direction-selective mechanisms per se, as Pack et al. (2005) found that neurons in macaque MT became less directional with increasing stimulus diameter for high-luminance stimuli but became more directional with increasing stimulus diameter for lower-luminance stimuli (see Fig. 3 of Pack et al. 2005).

DeValois and colleagues (De Valois and Cottaris 1998; De Valois et al. 2000) proposed that the two classes of nondirectional inputs that appear to be combined to generate direction-selective simple cells arise from the magno- and parvocellular subdivisions of the lateral

geniculate nucleus because mango-cellular responses tend to be fast and temporally biphasic, whereas parvocellular responses tend to be slower and temporally monophasic. Because parvocellular neurons generally have a lower contrast sensitivity than magnocellular neurons (Shapley et al. 1981), lowering contrast would be expected to selectively eliminate the parvocellular, or temporally monophasic, part of the response, which would, in turn, predict that responses should become more biphasic, not less, as observed. The finding that at low contrast the space-time slant becomes more vertical and tends not to fully invert phase therefore speaks against a model of direction selective simple cells being generated by combining magnocellular and parvocellular inputs.

ACKNOWLEDGMENTS

D. Freeman did the programming; T. Chuprina provided technical assistance. We thank Dr. Christopher Pack for advice and Matlab code.

GRANTS

This work was supported by National Eye Institute Grant EY-13135 and the Harvard Society of Fellows.

REFERENCES

Adelson EH, Bergen JR. Spatiotemporal energy models for the perception of motion. J Opt Soc Am [A] 1985;2:284–299.

Anderson JC, Binzegger T, Martin KA, Rockland KS. The connection from cortical area V1 to V5: a light and electron microscopic study. J Neurosci 1998;18:10525–10540. [PubMed: 9852590]

Anderson JC, Martin KA. Connection from cortical area V2 to MT in macaque monkey. J Comp Neurol 2002;443:56–70. [PubMed: 11793347]

Anzai A, Ohzawa I, Freeman RD. Joint-encoding of motion and depth by visual cortical neurons: neural basis of the Pulfrich effect. Nat Neurosci 2001;4:513–518. [PubMed: 11319560]

Baker CL Jr. Linear filtering and nonlinear inteactions in direction-selective visual cortex neurons: a noise correlation analysis. Vis Neurosci 2001;18:465–485. [PubMed: 11497423]

Benardete EA, Kaplan E. The dynamics of primate M retinal ganglion cells. Vis Neurosci 1999;16:355–368. [PubMed: 10367969]

Carandini M, Heeger DJ, Movshon JA. Linearity and normalization in simple cells of the macaque primary visual cortex. J Neurosci 1997;17:8621–8644. [PubMed: 9334433]

Cavanagh P, Tyler CW, Favreau OE. Perceived velocity of moving chromatic gratings. J Opt Soc Am [A] 1984;1:893–899.

Conway BR, Livingstone MS. Space-time maps and two-bar interactions of different classes of direction-selective cells in macaque V-1. J Neurophysiol 2003;89:2726–2742. [PubMed: 12740411]

De Valois RL, Cottaris NP. Inputs to directionally selective simple cells in macaque striate cortex. Proc Natl Acad Sci USA 1998;95:14488–14493. [PubMed: 9826727]

De Valois RL, Cottaris NP, Mahon LE, Elfar SD, Wilson JA. Spatial and temporal receptive fields of geniculate and cortical cells and directional selectivity. Vision Res 2000;40:3685–3702. [PubMed: 11090662]

DeAngelis GC, Ohzawa I, Freeman RD. Spatiotemporal organization of simple-cell receptive fields in the cat's striate cortex. I. General characteristics and postnatal development. J Neurophysiol 1993a; 69:1091–1117. [PubMed: 8492151]

DeAngelis GC, Ohzawa I, Freeman RD. Spatiotemporal organization of simple-cell receptive fields in the cat's striate cortex. II. Linearity of temporal and spatial summation. J Neurophysiol 1993b; 69:1118–1135. [PubMed: 8492152]

Dougherty RF, Press WA, Wandell BA. Perceived speed of colored stimuli. Neuron 1999;24:893–899. [PubMed: 10624952]

Gaska JP, Jacobson LD, Chen HW, Pollen DA. Space-time spectra of complex cell filters in the macaque monkey: a comparison of results obtained with pseudowhite noise and grating stimuli. Vis Neurosci 1994;11:805–821. [PubMed: 7918230]

Hubel DH. Tungsten microelectrode for recording from single units. Science 1957;125:549–550. [PubMed: 17793797]

Hubel DH, Wiesel TN. Receptive fields, binocular interaction and functional architecture in the cat's visual cortex. J Physiol 1962;160:106–154. [PubMed: 14449617]

Hubel DH, Wiesel TN. Laminar and columnar distribution of geniculocortical fibers in the macaque monkey. J Comp Neurol 1972;146:421–450. [PubMed: 4117368]

Judge SJ, Richmond BJ, Chu FC. Implantation of magnetic search coils for measurement of eye position: an improved method. Vision Res 1980;20:535–538. [PubMed: 6776685]

Krekelberg B, van Wezel RJ, Albright TD. Interactions between speed and contrast tuning in the middle temporal area: implications for the neural code for speed. J Neurosci 2006;26:8988–8998. [PubMed: 16943555]

Ledgeway T, Zhan C, Johnson AP, Song Y, Baker CL Jr. The direction-selective contrast response of area 18 neurons is different for first- and second-order motion. Vis Neurosci 2005;22:87–99. [PubMed: 15842744]

Livingstone MS. Mechanisms of direction selectivity in macaque V1. Neuron 1998;20:509–526. [PubMed: 9539125]

Livingstone MS. Two-bar interactions in space and time: evidence for common mechanisms in stereopsis and direction selectivity. Soc Neurosci Abstr 1999;25:1934.

Livingstone MS, Conway BR. Substructure of direction-selective receptive fields in macaque V1. J Neurophysiol 2003;89:2743–2759. [PubMed: 12740412]

Livingstone MS, Pack CC, Born RT. Two-dimensional substructure of MT receptive fields. Neuron 2001;30:781–793. [PubMed: 11430811]

Lund JS. Organization of neurons in the visual cortex, area 17, of the monkey (*Macaca mulatta*). J Comp Neurol 1973;147:455–496. [PubMed: 4122705]

Maunsell JH, Ghose GM, Assad JA, McAdams CJ, Boudreau CE, Noerager BD. Visual response latencies of magnocellular and parvocellular LGN neurons in macaque monkeys. Vis Neurosci 1999;16:1–14. [PubMed: 10022474]

Maunsell JH, Gibson JR. Visual response latencies in striate cortex of the macaque monkey. J Neurophysiol 1992;68:1332–1344. [PubMed: 1432087]

McLean J, Palmer LA. Contribution of linear spatiotemporal receptive field structure to velocity selectivity of simple cells in area 17 of cat. Vision Res 1989;29:675–679. [PubMed: 2626824]

McLean J, Raab S, Palmer LA. Contribution of linear mechanisms to the specification of local motion by simple cells in areas 17 and 18 of the cat. Vis Neurosci 1994;11:271–294. [PubMed: 8003454]

Mikami A, Newsome WT, Wurtz RH. Motion selectivity in macaque visual cortex. II. Spatiotemporal range of directional interactions in MT and V1. J Neurophysiol 1986;55:1328–1339. [PubMed: 3734858]

Movshon JA, Newsome WT. Visual response properties of striate cortical neurons projecting to area MT in macaque monkeys. J Neurosci 1996;16:7733–7741. [PubMed: 8922429]

Nover H, Anderson CH, DeAngelis GC. A logarithmic, scale-invariant representation of speed in macaque middle temporal area accounts for speed discrimination performance. J Neurosci 2005;25:10049–10060. [PubMed: 16251454]

Pack CC, Born RT, Livingstone MS. Two-dimensional substructure of stereo and motion interactions in macaque visual cortex. Neuron 2003;37:525–535. [PubMed: 12575958]

Pack CC, Conway BR, Born RT, Livingstone MS. Spatiotemporal structure of nonlinear subunits in macaque visual cortex. J Neurosci 2006;26:893–907. [PubMed: 16421309]

Pack CC, Hunter JN, Born RT. Contrast dependence of suppressive influences in cortical area MT of alert macaque. J Neurophysiol 2005;93:1809–1815. [PubMed: 15483068]

Peterson MR, Li B, Freeman RD. The derivation of direction selectivity in the striate cortex. J Neurosci 2004;24:3583–3591. [PubMed: 15071106]

Peterson MR, Li B, Freeman RD. Direction selectivity of neurons in the striate cortex increases as stimulus contrast is decreased. J Neurophysiol 2006;95:2705–2712. [PubMed: 16306177]

Peterson M, Ohzawa I, Freeman R. Neural and perceptual adjustments to dim light. Vis Neurosci 2001;18:203–208. [PubMed: 11417795]

Priebe NJ, Lisberger SG, Movshon JA. Tuning for spatiotemporal frequency and speed in directionally selective neurons of macaque striate cortex. J Neurosci 2006;26:2941–2950. [PubMed: 16540571]

Purpura K, Tranchina D, Kaplan E, Shapley RM. Light adaptation in the primate retina: analysis of changes in gain and dynamics of monkey retinal ganglion cells. Vis Neurosci 1990;4:75–93. [PubMed: 2176096]

Ramoa AS, Freeman RD, Macy A. Comparison of response properties of cells in the cat's visual cortex at high and low luminance levels. J Neurophysiol 1985;54:61–72. [PubMed: 4031982]

Reich DS, Mechler F, Victor JD. Temporal coding of contrast in primary visual cortex: when, what, and why. J Neurophysiol 2001;85:1039–1050. [PubMed: 11247974]

Rockland KS. Visual cortical organization at the single axon level: a beginning. Neurosci Res 2002;42:155–166. [PubMed: 11900825]

Sestokas AK, Lehmkuhle S. Visual response latency of X- and Y-cells in the dorsal lateral geniculate nucleus of the cat. Vision Res 1986;26:1041–1054. [PubMed: 3798741]

Shapley R, Kaplan E, Soodak R. Spatial summation and contrast sensitivity of X and Y cells in the lateral geniculate nucleus of the macaque. Nature 1981;292:543–545. [PubMed: 7254350]

Shapley RM, Victor JD. The effect of contrast on the transfer properties of cat retinal ganglion cells. J Physiol 1978;285:275–298. [PubMed: 745079]

Snowden RJ, Stimpson N, Ruddle RA. Speed perception fogs up as visibility drops. Nature 1998;392:450. [PubMed: 9548251]

Stone LS, Thompson P. Human speed perception is contrast dependent. Vision Res 1992;32:1535–1549. [PubMed: 1455726]

Thompson P, Brooks K, Hammett ST. Speed can go up as well as down at low contrast: implications for models of motion perception. Vision Res 2006;46:782–786. [PubMed: 16171842]

Tsao DY, Conway BR, Livingstone MS. Receptive fields of disparity-tuned simple cells in macaque V1. Neuron 2003;38:103–114. [PubMed: 12691668]

Van Wezel RJ, Krekelberg B, Albright TD. Linking macaque area MT neural acivity to speed perception. Soc Neurosci Abstr 2003;33:591–594.

Watson AB, Ahumada AJ Jr. Model of human visual-motion sensing. J Opt Soc Am [A] 1985;2:322–341.

Yabuta NH, Sawatari A, Callaway EM. Two functional channels from primary visual cortex to dorsal visual cortical areas. Science 2001;292:297–300. [PubMed: 11303106]

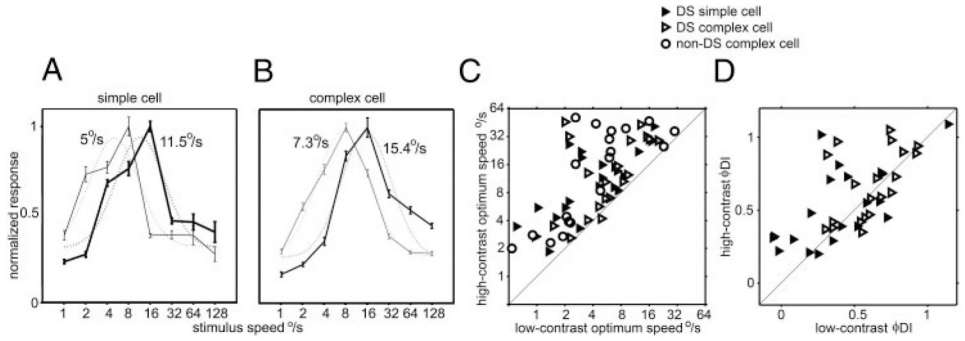

FIG. 1.

Speed tuning at low- and high-contrast in alert macaque V1. *A*: speed tuning of a V1 directional simple cell measured using high (thick lines) and low (thin lines) contrast stimuli. Dotted lines are the log-Gaussian fit to the data; the optimum speed tuning, taken from the center of the log-Gaussian, is indicated for each curve. *B*: same as *A* for a V1 complex cell. *C*: scatter plot of the speed tuning of 21 directional simple cells (open triangles), 22 directional complex cells (filled triangles), and 19 nondirectional complex cells for high- and low-contrast stimuli. *D*: scatter plot of direction indices of direction-selective simple and complex cells to phi motion stimuli (flashed sequential pairs of bars in a sparse noise stimulus) for high- and low-contrast stimuli.

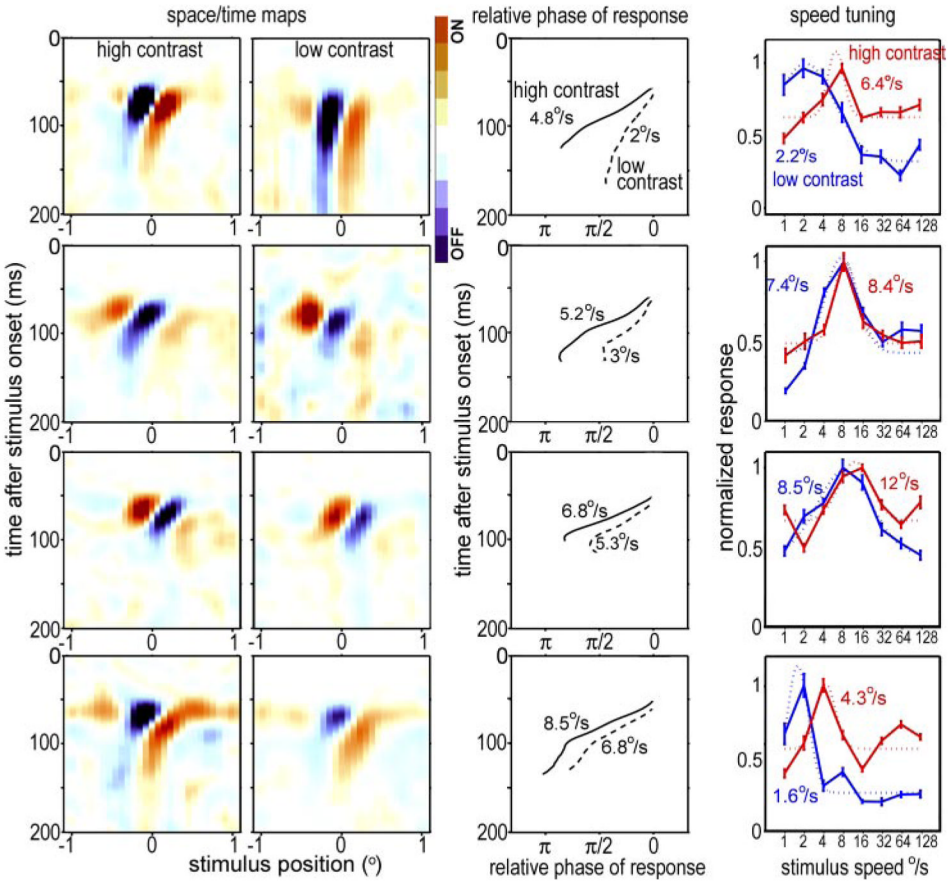

FIG. 2.

Space-time maps, relative response phase as a function of time after stimulus onset, and speed tuning for 4 V1 directional simple cells. Each row shows data for 1 cell. *Left 2 columns*: space-time maps (light minus dark responses) as a function of time after stimulus onset and stimulus position along the stimulus range, for high-contrast (*far left*) and low-contrast (*2nd column*) stimuli. Each map is normalized to the maximum average response (either light excitatory, or ON, or dark excitatory, or OFF). *Third column*: phase of a Gabor, fit to the response (relative to response onset), as a function of time after stimulus onset. *Right*: speed tuning of each cell at high and low contrasts; dotted lines are the log-Gaussians fit to the data. The optimum speeds, taken from the centers of the log-Gaussians are indicated for each curve.

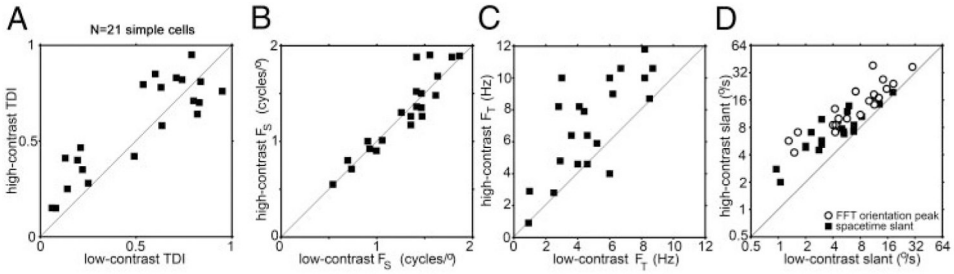

FIG. 3.

Simple-cell spatial and temporal response characteristics for high- and low-contrast stimuli. *A*: tilt direction index for 21 simple cells for high- and low-contrast stimuli. The tilt direction index reflects the degree of asymmetry in the space-time map. *B*: optimal spatial frequency, derived from the spatial frequency peak of the 2-D Fourier transform of the space-time map, for 21 simple directional cells. *C*: optimal temporal frequency, derived from the temporal frequency peak of the 2-D Fourier transform of the space-time map, for 21 simple directional cells. *D*: slant of the space-time maps at high and low contrast, measured from the slope of phase vs. time (■) or from the maximum spatial-frequency/temporal-frequency orientation in the fast Fourier transform (FFT). Most of the simple cells showed slants that predicted faster optimum speeds at high contrast than at low; i.e., they are above the $x = y$ diagonal.

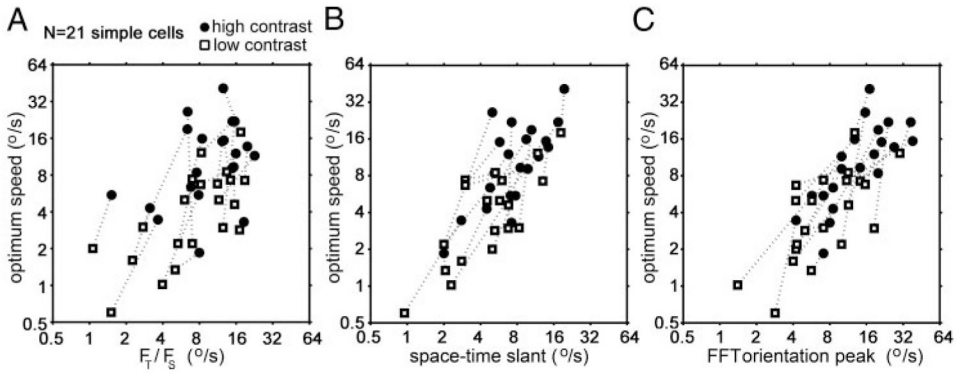

FIG. 4.

Correlations between actual speed tuning (vertical axis) and different ways of predicting the optimal speed from the spatiotemporal characteristics of the space-time maps. Each pair of connected points corresponds to data for 1 cell. *A*: optimum speed vs. optimum speed predicted from the ratio of the optimum temporal frequency to optimum spatial frequency. *B*: optimum speed vs. optimum speed predicted from the space-time slant measured from the slope of the response phase as a function of time. *C*: optimum speed vs. optimum speed predicted from the peak orientation in temporal frequency/spatial frequency of the Fourier transform of the space-time map.

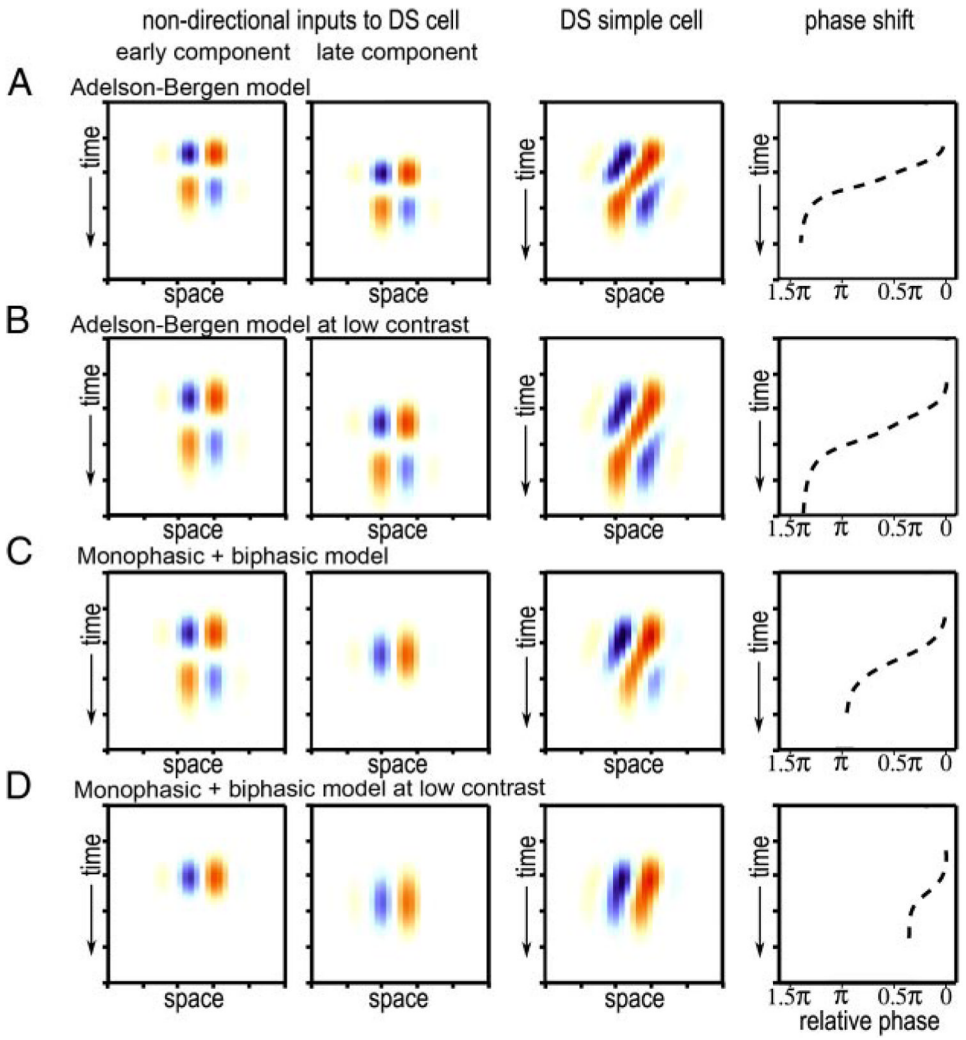

FIG. 5.

Space-time maps and phase shifts for high- and low-contrast stimuli for 2 different models for generating direction-selective simple cells. See text for details.